Proceedings of the Sixteenth International Conference on
Computational Structures Technology
Edited by: P. Iványi, J. Kruis and B.H.V. Topping
Civil-Comp Conferences, Volume 14, Paper 2.4
Civil-Comp Press, Edinburgh, United Kingdom, 2026
ISSN: 2753-3239, doi: 10.4203/ccc.14.2.4

An Impact of the FETI Gluing Conditions on Dual Operator Conditioning and Convergence Rate

A. Růžička[1,2], D. Horák[1,2] and J. Kružík[1,2]

[1] Department of Applied Mathematics, Faculty of Electrical Engineering and Computer Science, VSB - Technical University of Ostrava, Czechia
[2] Institute of Geonics, Czech Academy of Sciences, Ostrava, Czechia

Abstract

FETI-type domain decomposition methods are one of the most effective solvers for systems of linear equations, e.g. those arising during FEM-discretization of problems from mechanics. The main idea is to decompose the domain of interest into non-overlapping subdomains, including doubling nodes at subdomain interfaces, "gluing" these doubled nodes using Lagrange multipliers, and then eliminating the primary unknowns. For simplicity, we will stick to the problem of 2D linear elasticity. Gluing conformally discretized subdomains is straightforward for doubled nodes and leads to rows in the gluing matrix containing two non-zero values: 1 and -1. These rows of the gluing matrix are usually normalized. However, a problem arises for the nodes lying in the place where 4 neigbouring subdomains meet in one point. There exist a number of ways of gluing degrees of freedom belonging to these nodes. This paper investigates variants of interconnecting corresponding quartets of coincident subdomain corners for the 2D decomposed, FEM-discretized, problem of linear elasticity. Both the convergence and spectral properties (conditioning) of the corresponding dual operators for each variant of interconnection for TFETI and for HTFETI, for 2 ways of aggregation of subdomains in larger complexes called clusters, are compared.

Keywords: FETI method, domain decomposition, convergence, dual operator conditioning, gluing conditions, corner nodes quartets, aggregation into clusters

1 Introduction - 2D Linear Elastic Model Problem, TFETI and HTFETI

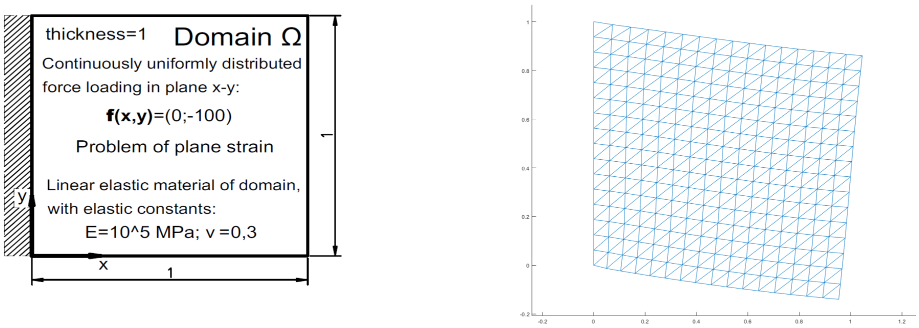

(a) Definition of the problem

(b) Solution of the problem

Figure 1: The benchmark: 2D problem of linear elasticity

Let us start with an introduction to the benchmark problem which was used in all numerical experiments whose results are presented in the paper. The model 2D linear elasticity problem, depicted in Figure 1a, defined on a 2D linear elastic domain and fixed against motion as an absolutely rigid body along its left edge, was chosen. The domain is decomposed into $(1/H)^2$ identical square non-overlapping subdomains with edge length H. The subdomains are uniformly discretized by identical 2D finite elements in the shape of an isosceles right-angled triangle with leg length h, with a discretization ratio of the subdomains of H/h by finite elements along their edges.

The illustration of the discretization of the domain and of the problem solution, i.e., of how the decomposed discretized domain deforms, is given in Figure 1b.

1.1 Set parameters of numerical experiments

In all presented experiments, the domain was decomposed into $16 \cdot 16$ identical square subdomain of the edge length $H = 1/16$. In all experiments, the rows of the gluing (constraint) matrix B (of the matrices B_0 and B_1 in HTFETI) were normalized to the unit norm.

The resulting obtained system of linear equations given by Equation 1:

$$Ax = b, \tag{1}$$

where $A = PFP$ and $b = d - F\lambda_0$ for TFETI 1 (see [2]), or $A = \tilde{P}\tilde{F}\tilde{P}$ and $b = \tilde{d} - \tilde{F}\tilde{\lambda}_0$ (see e.g. [5]) for is solved by the conjugate gradient (CG) method.

The stopping criterion of the CG method is the decrease in the relative residual norm $||r_k|| \leq \epsilon ||b||$, where: $\epsilon = 10^{-6}$. All numerical experiments were performed in Matlab.

2 Gluing conditions

The continuity of the entire decomposed domain during its deformation on the outside has to be ensured by performing so-called gluing on subdomain interfaces.

The gluing is mathematically realized by introducing the problem constraints in form: $Bu = o$, with $B \in \mathbb{R}^{m\times n}$ as the gluing (constraint) matrix, which ensures continuity of the values of nodal displacements.

In case of (quasi)static problem of linear elasticity, i.e. with the entire decomposed domain prevented from its free motion as one absolutely rigid body, represented by identical rigid body motion of each subdomain, the gluing conditions together with the Dirichlet BCs of the problem ensure the uniqueness of the problem solution.

2.1 Gluing conditions for pairs of nodes

Pairs of coincident nodes from two different subdomains appear on the shared edge interface of the subdomains, and, for the outermost subdomains placed along the boundary of the entire decomposed domain, they also appear at corners of these subdomains lying on that boundary.

The condition that equates the values of two coincident nodes i and j on opposite sides of the interface of two subdomains is expressed as $u_i - u_j = 0$. The row of B realizing this condition in the constraints $Bu = o$ is thus a boolean vector with 1 at position i and -1 at position j.

The equality has to be ensured for all deformation parameters that these coincident nodes have, i.e., for a 2D problem of linear elasticity, for both the x- and y-component of displacement. Thus, the block of the matrix B, which in $Bu = o$, sets the value of both displacement components for nodes i and j has the following structure:

$$\begin{array}{c} \begin{array}{ccccccc} & i_x & i_y & & j_x & j_y & \end{array} \\ \begin{bmatrix} o & 1 & 0 & o & -1 & 0 & o \\ o & 0 & 1 & o & 0 & -1 & o \end{bmatrix} \end{array}. \tag{2}$$

2.2 Gluing conditions for quartets of nodes

Quartets of coincident corner nodes of four neighbouring subdomains meeting at one point appear only in the interior of the decomposed domain. The most commonly used method of interconnecting these corner quartets is the case where the rows of the gluing matrix B are orthogonal. A total of four ways of interconnecting the quartets of subdomains' corner nodes by the method with orthogonal rows of B exist; see Table 1 and corresponding rows of matrix B in Table 2.

When the rows of the gluing matrix B are normalized to the unit norm, all four presented interconnection variants are spectrally equivalent. This spectral equivalence holds because the matrix B for any given variant can be obtained by premultiplying the matrix B of another variant by a corresponding orthogonal transformation matrix.

A.1	A.2	A.3	A.4
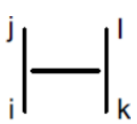	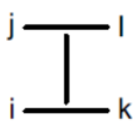	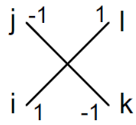	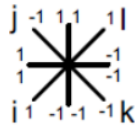

Table 1: Ways of interconnecting of coincident subdomain corners quartets (setting values of their deformation parameters equal) for B with orthogonal rows

A.1	A.2
$\begin{array}{c} \begin{array}{ccccccccccccc} & i_x & i_y & & j_x & j_y & & k_x & k_y & & l_x & l_y & \end{array} \\ \begin{bmatrix} o & 1 & 0 & o & 1 & 0 & o & -1 & 0 & o & -1 & 0 & o \\ o & 0 & 1 & o & 0 & 1 & o & 0 & -1 & o & 0 & -1 & o \\ o & -1 & 0 & o & 1 & 0 & o & 0 & 0 & o & 0 & 0 & o \\ o & 0 & -1 & o & 0 & 1 & o & 0 & 0 & o & 0 & 0 & o \\ o & 0 & 0 & o & 0 & 0 & o & -1 & 0 & o & 1 & 0 & o \\ o & 0 & 0 & o & 0 & 0 & o & 0 & -1 & o & 0 & 1 & o \end{bmatrix} \end{array}$	$\begin{array}{c} \begin{array}{ccccccccccccc} & i_x & i_y & & j_x & j_y & & k_x & k_y & & l_x & l_y & \end{array} \\ \begin{bmatrix} o & -1 & 0 & o & 1 & 0 & o & -1 & 0 & o & 1 & 0 & o \\ o & 0 & -1 & o & 0 & 1 & o & 0 & -1 & o & 0 & 1 & o \\ o & 1 & 0 & o & 0 & 0 & o & -1 & 0 & o & 0 & 0 & o \\ o & 0 & 1 & o & 0 & 0 & o & 0 & -1 & o & 0 & 0 & o \\ o & 0 & 0 & o & 1 & 0 & o & 0 & 0 & o & -1 & 0 & o \\ o & 0 & 0 & o & 0 & 1 & o & 0 & 0 & o & 0 & -1 & o \end{bmatrix} \end{array}$
A.3	**A.4**
$\begin{array}{c} \begin{array}{ccccccccccccc} & i_x & i_y & & j_x & j_y & & k_x & k_y & & l_x & l_y & \end{array} \\ \begin{bmatrix} o & 1 & 0 & o & -1 & 0 & o & -1 & 0 & o & 1 & 0 & o \\ o & 0 & 1 & o & 0 & -1 & o & 0 & -1 & o & 0 & 1 & o \\ o & 1 & 0 & o & 0 & 0 & o & 0 & 0 & o & -1 & 0 & o \\ o & 0 & 1 & o & 0 & 0 & o & 0 & 0 & o & 0 & -1 & o \\ o & 0 & 0 & o & 1 & 0 & o & -1 & 0 & o & 0 & 0 & o \\ o & 0 & 0 & o & 0 & 1 & o & 0 & -1 & o & 0 & 0 & o \end{bmatrix} \end{array}$	$\begin{array}{c} \begin{array}{ccccccccccccc} & i_x & i_y & & j_x & j_y & & k_x & k_y & & l_x & l_y & \end{array} \\ \begin{bmatrix} o & 1 & 0 & o & 1 & 0 & o & -1 & 0 & o & -1 & 0 & o \\ o & 0 & 1 & o & 0 & 1 & o & 0 & -1 & o & 0 & -1 & o \\ o & -1 & 0 & o & 1 & 0 & o & -1 & 0 & o & 1 & 0 & o \\ o & 0 & -1 & o & 0 & 1 & o & 0 & -1 & o & 0 & 1 & o \\ o & 1 & 0 & o & -1 & 0 & o & -1 & 0 & o & 1 & 0 & o \\ o & 0 & 1 & o & 0 & -1 & o & 0 & -1 & o & 0 & 1 & o \end{bmatrix} \end{array}$

Table 2: The rows of B formulating the constraints setting equal values of x and y-component of displacement of corresponding quartet of coincident subdomain corner nodes for B with orthogonal rows for 2D linear elasticity

However, 11 other interconnection variants for these coincident corner quartets exist. In these variants, the displacements are equated only between specific node pairs (m, n), where $m, n \in \{i, j, k, l\}$. This is done similarly to pairs on opposite sides of a shared edge interface, using equations of the form $u_m - u_n = 0$. These constraints may be linearly dependent but no constraint is a multiple of other constraints in the set. Therefore, these variants can be categorized by their number of redundant (linearly dependent) constraints. This redundancy is measured against the minimum of three constraints required to equate a single deformation parameter across the quartet.

The 12 interconnection variants (including the orthonormal cases as a single variant) are shown in Table 3, where the link between a corresponding pair of nodes indicates that the values of the displacements for this pair are set equal by a corresponding pair of constraints.

Variants of interconnection of corner nodes quartets without redundant constraints				
Ortogonal rows of B (A)	Connection into Z (B)	Connection into U (C)	Star (D)	Hourglass without top (E)
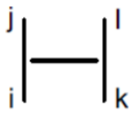	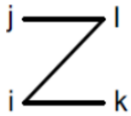	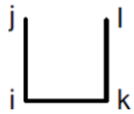	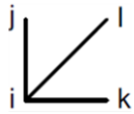	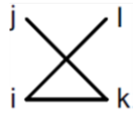
Variants of interconnection of corner quartets with 1 redundant constraint				
Rectangle (F)	Hourglass (G)	Arrow (H)	$\triangle$ with tail (I)	
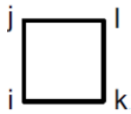	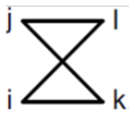	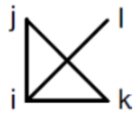	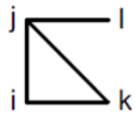	
Variants with 2 redundant constraint			Variants with 3 redundant constraints	
Fully redundant connect. without diagonal (J)	Fully redundant connect. without edge (K)		Fully redundant connection (L)	
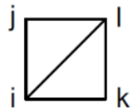	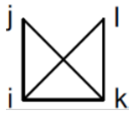		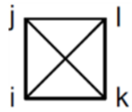	

Table 3: Tested variants of interconnecting quartets of coincident subdomain corners

Excluding the cases denoted as A, B, F, I, and L, the presented variants have subvariants given by only rotating the notional diagram (pattern, graph) presented in Table 3. There are four possible rotations of the diagram for these corresponding cases, i.e., by $0°$, $90°$, $180°$, and $270°$ (2 rotations by $0°$, $90°$ for cases G and J) For cases B and I (the connection into Z and into the triangle with a tail), there are two possible mirror images, where each mirror image has two possible rotations of the diagram by $0°$ and $90°$ for case B, and four possible rotations by $0°$, $90°$, $180°$, and $270°$ for case I.

The spectral properties of the corresponding operators in both TFETI ($F = BK^{+}B^{T}$ and $A = PFP$) and HTFETI ($\tilde{F} = \tilde{B}\tilde{K}^{+}\tilde{B}^{T}$ and $A = \tilde{P}\tilde{F}\tilde{P}$), and thus also the convergence properties for each variant of interconnecting corresponding quartets of coincident corner nodes, can differ significantly.

3 Spectral properties of TFETI operators

The nonzero part of the spectra of $F = BK^{+}B^{T}$ and $A = PFP$ for TFETI (for more information about (T)FETI and F and A see e.g. [1] or [2]) for each variant of interconnecting quartets obtained for the benchmark problem, presented in Figure 1 for $H = 1/16$ and $H/h = 8$, is shown in Figure 3.

The charts correspond to the case where each variant is represented by its subvariant with the diagram of the node interconnection in its standard state, without rotation or orientation change, as presented in Table 3.

The color scale used in the presented charts for each particular series representing a corresponding variant of interconnecting quartets is depicted in Figure 2.

Figure 2: Color scale used in the charts of spectra of $F = BK^{+}B^{T}$ and $A = PFP$

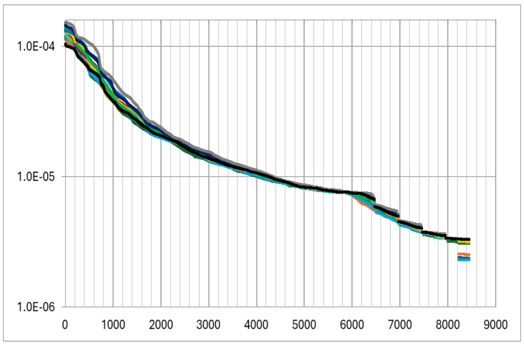

(a) Entire nonzero part of the spectrum of F with y-axis in logarithmic scale

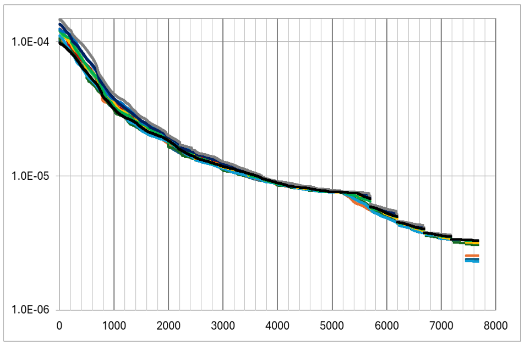

(b) Nonzero part of the spectrum of A for with y-axis in logarithmic scale

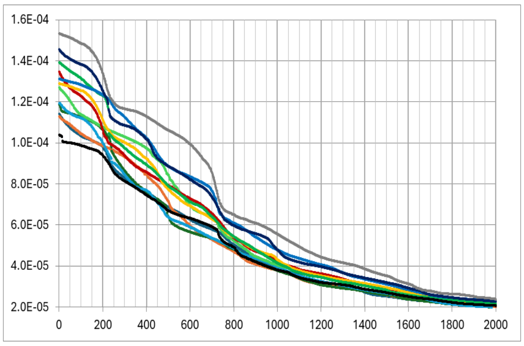

(c) Detail of the nonzero part of the spectrum of F for 2000 highest eigenvalues

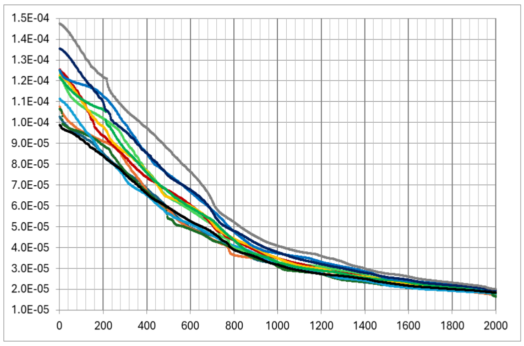

(d) Detail of the nonzero part of the spectrum of A for 2000 highest eigenvalues

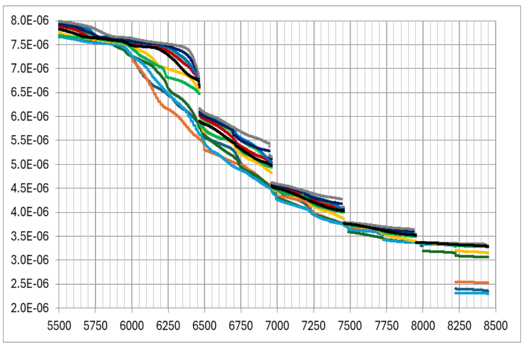

(e) Detail of the spectrum of F for 2949 lowest nonzero eigenvalues

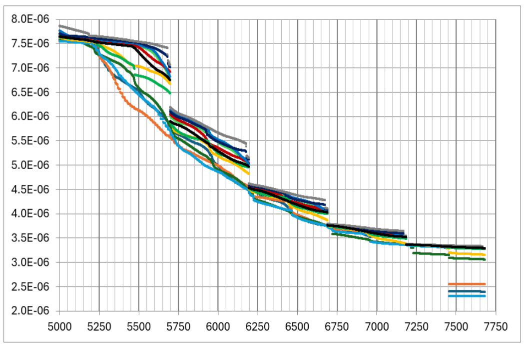

(f) Detail of the spectrum of A for the 2681 lowest nonzero eigenvalue

Figure 3: Spectra of F and A TFETI operators

The corresponding regular condition number κ^{reg} of the operator F and of the system matrix A are presented in the Table 4.

	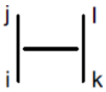	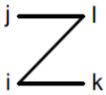	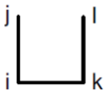	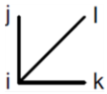	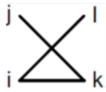	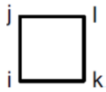
	A	B	C	D	E	F
$F = BK^{+}B^{T}$	31.5	48.5	44.8	38.8	51.9	38.5
$A = PFP$	30.0	42.8	42.2	34.7	48.2	38.0
	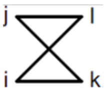	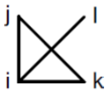	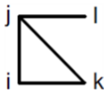	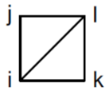	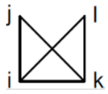	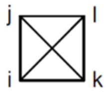
	G	H	I	J	K	L
$F = BK^{+}B^{T}$	40.9	40.9	42.5	39.8	44.2	46.5
$A = PFP$	38.0	38.8	37.1	38.0	41.2	44.7

Table 4: Conditioning of $F = BK^{+}B^{T}$ and $A = PFP$ for TFETI for each tested variant of interconnecting quartets of corners for $H = 1/16, H/h = 8$

From the charts in Fig. 3 and from the Table 4 following conclusions can be made:

The conditioning was the best for the case A with orthonormal rows of B and the worst for the case E of interconnection into hourglass without top.

The line L representing the nonzero part of the spectra of F and A for the fully redundant variant of interconnecting corresponding quartets of coincident corners of 4 neighbouring subdomains forms for the upper envelope of the charts for all variants of interconnection for both operators, i.e. for the fully redundant case the given ith highest eigenvalue of the operator is always highest among all variants .

The lines representing the spectra of F and A for the variants of interconnection where setting the values of corresponding one of displacement components of the corners is mathematically formulated with the same number of redundant constraints form bundles of mutually interwining lines, by contrast, the series from the different bundles hardly ever interwine each other. The cases of interconnection A with orthonormal rows of B and the fully redundant variant H form each their solitary bundle.

The variants of interconnection with more redundant constraints have the values of the corresponding ith highest eigenvalue higher than those with less constraints.

The first bundle is formed by the lines representing the nonzero part of the spectra for the cases of interconnection with no redundant constraints, except for the case A with orthonormal rows of B, where, however, for the case D circa 225 lowest nonzero eigenvalues are circa 1.3-times higher than for the cases B, C, E. On the other hand, circa 225 previous higher eigenvalues for case D are slightly lower than for B, C, E.

The bundle for the cases with 1 redundant constraint are actually 2 boundles with the first one for the cases H and I where especially the lowest nonzero eigenvalues are slightly lower than for F, G, J, K, L and the second one with the cases F and G where the lowest eigenvalues are almost equal to those for cases with 2 or 3 redundant constraints, with highest eigenvalues altogether, where especially the line representing the spectra for the case F of rectangle shape, interwines with the spectra of the operators for the cases J, K with 2 redundant constraints.

The nonzero part of the spectra of the operators $F = BK^{+}B^{T}$ and $A = PFP$ for the case A, where the constraints equating displacement components of corner quartet were formulated using matrix B with orthonormal rows acts differently than for the remaining cases of interconnection with given number of redundant constraints.

The highest eigenvalues of both F and A are for the case A with orthonormal rows of B the lowest among all variants of quartets interconnection. Then it gradually crosses the bundles representing the spectra of F or A for the other case with no redundant constraints and then also the bundle for the cases H, I, until the eigenvalues become almost equal to the value of the lowest nonzero eigenvalues for the cases F, G, J, K, L, which have the highest values of the lowest nonzero eigenvalues altogether.

This course of spectra together with having the lowest condition number of both $F = BK^{+}B^{T}$ and $A = PFP$, shows that the variant with orthonormal rows of matrix B is spectrally optimal and should also have the optimal convergence properties.

This distribution of the spectra into bundles is actually related to spectral graph theory, where the block of the gluing matrix B formulating the constraints setting the values of displacement of the node quartet equal is identified with the incidence matrix of the graph representing the corresponding variant of interconnection, see more in [3].

4 Convergence properties

4.1 TFETI

In this section, the 12 variants, which were presented in Table 3 and whose corresponding spectral properties, resp. conditioning, were compared in Figure 3, resp. in Table 4, are compared in terms of their convergence properties. Table 4 presents the number of CG iterations for TFETI for the benchmark presented in Section 1. The CG iteration numbers are presented for all possible orientations of the notional diagram of interconnection, i.e., all possible rotations (clockwise) and mirrorings.

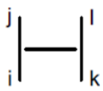		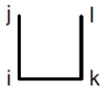	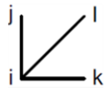	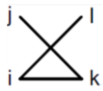	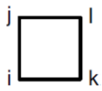
A	B	C	D	E	F
33/ 33/ 33/ 33	37/ 39 // 38/ 38	38/ 38/ 38/ 39	35/ 35/ 34/ 35	39/ 40/ 39/ 40	38
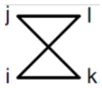	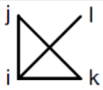	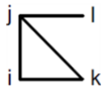	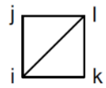	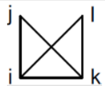	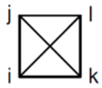
G	H	I	J	K	L
37/ 37	36/ 38/ 37/ 38	37/ 36/ 37/ 36 // 37/ 37/ 37/ 36	37/ 38	38/ 38/ 38/ 38	39

Table 5: Numbers of CG iterations for TFETI for each variant of interconnecting quartets of subdomain corners, for $H = 1/16, H/h = 8$

From the presented results, it follows that the interconnection using orthonormal rows (variant A) is also optimal in terms of its convergence properties. The only variant that can match A to some degree is the interconnection into a star (variant D). On the other hand, the worst results were obtained for cases E and L, i.e., the interconnection into an hourglass without a top, and the fully redundant case.

4.2 HTFETI

Numerical experiments on the benchmark presented in Section 1 were also performed for HTFETI method. In this method the corresponding groups of subdomains are aggregated into larger clusters acting as one absolutely rigid body. This aggregation is performed by partially connecting the neighbouring subdomains in clusters on the primal variables level by means of enforcing:

- continuity of displacements in subdomain corners in the cluster,
- equality of averages of nodal displacement components on opposite sides of subdomains' interfaces in the cluster and of averages of rotations of the nodes around given reference point due to these displacements (more in [7]).

Table 6 presents the numbers of CG iterations for TFETI and HTFETI. Experiments were performed for all 12 variants of corner interconnections (including all orientations) on the benchmark presented in Section 1. For HTFETI, the results are presented for cases with clusters consisting of $2 \cdot 2$ and $4 \cdot 4$ subdomains. Table 7 presents the corresponding largest and smallest nonzero eigenvalues ($\lambda_{max}, \lambda_{min}^{reg}$) and the regular condition number κ^{reg} for the cases with the diagrams of interconnection of the quartets in their standard state (position) as it is given in Table 3.

Again, the gluing of corners using orthonormal rows results in the lowest number of CG iterations even for HTFETI. Moreover, the method using averaging and moment equilibrium to aggregate the subdomains into clusters gives a significantly lower number of iterations than using continuity of displacement in the corners.

			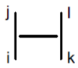	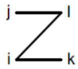	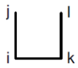	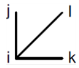	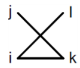	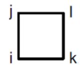
			A	B	C	D	E	F
TFETI			33/33/33/33	37/39//38/38	38/38/38/39	35/35/34/35	39/40/39/40	38
HTFETI	aver.+mom.	$2 \cdot 2$ sub.	54/54/54/54	63/60//59/63	62/62/62/62	56/57/56/57	63/63/63/63	57
		$4 \cdot 4$ sub.	82/82/82/82	96/92//90/98	94/92/93/91	87/87/86/86	98/97/98/97	83
	corners	$2 \cdot 2$ sub.	68/68/68/68	75/72//73/75	76/76/76/75	70/69/70/69	75/76/76/75	72
		$4 \cdot 4$ sub.	101/102/100/102	112/105/105/114	110/110/110/109	103/102/102/102	114/114/114/114	102
			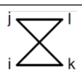	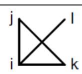	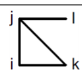	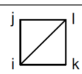	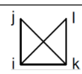	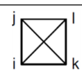
			G	H	I	J	K	L
TFETI			37/37	36/38/37/38	37/36/37/36// 37/37/37/36	37/38	38/38/38/38	39
HTFETI	aver.+mom.	$2 \cdot 2$ sub.	55/56	57/58/57/58	56/57/57/57// 57/57/56/57	57/57	57/56/57/57	58
		$4 \cdot 4$ sub.	86/87	90/91/88/91	86/89/86/89// 87/88/87/89	88/87	89/89/89/88	91
	corners	$2 \cdot 2$ sub.	69/69	69/70/69/69	71/71/71/71// 70/71/71/71	71/72	70/71/70/70	71
		$4 \cdot 4$ sub.	105/104	104/104/103/103	103/104/102/104// 103/104/103/103	105/104	106/105/106/105	107

Table 6: Number of CG iterations for TFETI and HTFETI with both tested methods of subdomain aggregation for each variant of interconnecting corresponding quartets of subdomain corners, for $H = 1/16, H/h = 8$

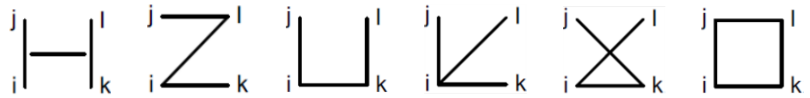

			A	B	C	D	E	F
TFETI		λ_{max}	$9.88\cdot10^{-5}$	$1.03\cdot10^{-4}$	$1.08\cdot10^{-4}$	$1.06\cdot10^{-6}$	$1.11\cdot10^{-4}$	$1.25\cdot10^{-4}$
		λ_{min}^{reg}	$3.29\cdot10^{-6}$	$2.40\cdot10^{-6}$	$2.55\cdot10^{-6}$	$3.06\cdot10^{-6}$	$2.31\cdot10^{-6}$	$3.29\cdot10^{-6}$
		κ^{reg}	30.0	42.8	42.2	34.7	48.2	38.0
HTFETI, averages + moments	$2\cdot2$ subd.	λ_{max}	$2.45\cdot10^{-4}$	$2.48\cdot10^{-4}$	$2.53\cdot10^{-4}$	$2.57\cdot10^{-4}$	$2.49\cdot10^{-4}$	$2.72\cdot10^{-4}$
		λ_{min}^{reg}	$3.29\cdot10^{-6}$	$2.40\cdot10^{-6}$	$2.55\cdot10^{-6}$	$3.07\cdot10^{-6}$	$2.31\cdot10^{-6}$	$3.29\cdot10^{-6}$
		κ^{reg}	74.5	103.4	99.0	83.7	107.6	82.7
	$4\cdot4$ subd.	λ_{max}	$6.43\cdot10^{-4}$	$6.44\cdot10^{-4}$	$6.33\cdot10^{-4}$	$6.64\cdot10^{-4}$	$6.68\cdot10^{-4}$	$6.68\cdot10^{-4}$
		λ_{min}^{reg}	$3.29\cdot10^{-6}$	$2.40\cdot10^{-6}$	$2.55\cdot10^{-6}$	$3.07\cdot10^{-6}$	$2.31\cdot10^{-6}$	$3.29\cdot10^{-6}$
		κ^{reg}	195.4	267.8	248.2	216.1	289.0	202.8
HTFETI, equality in corners	$2\cdot2$ subd.	λ_{max}	$4.70\cdot10^{-4}$	$4.67\cdot10^{-4}$	$4.86\cdot10^{-4}$	$4.79\cdot10^{-4}$	$4.63\cdot10^{-4}$	$5.13\cdot10^{-4}$
		λ_{min}^{reg}	$3.30\cdot10^{-6}$	$2.40\cdot10^{-6}$	$2.55\cdot10^{-6}$	$3.08\cdot10^{-6}$	$2.31\cdot10^{-6}$	$3.30\cdot10^{-6}$
		κ^{reg}	142.5	194.2	190.5	155.7	200.5	155.6
	$4\cdot4$ subd.	λ_{max}	$1.24\cdot10^{-3}$	$1.22\cdot10^{-3}$	$1.25\cdot10^{-3}$	$1.26\cdot10^{-3}$	$1.25\cdot10^{-3}$	$1.27\cdot10^{-3}$
		λ_{min}^{reg}	$3.29\cdot10^{-6}$	$2.40\cdot10^{-6}$	$2.55\cdot10^{-6}$	$3.07\cdot10^{-6}$	$2.31\cdot10^{-6}$	$3.29\cdot10^{-6}$
		κ^{reg}	377.6	509.6	488.2	409.8	539.3	385.9

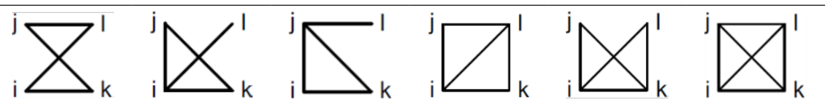

			G	H	I	J	K	L
TFETI		λ_{max}	$1.25\cdot10^{-4}$	$1.22\cdot10^{-4}$	$1.22\cdot10^{-4}$	$1.25\cdot10^{-4}$	$1.36\cdot10^{-4}$	$1.47\cdot10^{-4}$
		λ_{min}^{reg}	$3.29\cdot10^{-6}$	$3.16\cdot10^{-6}$	$3.28\cdot10^{-6}$	$3.29\cdot10^{-6}$	$3.29\cdot10^{-6}$	$3.30\cdot10^{-6}$
		κ^{reg}	38.0	38.8	37.1	38.0	41.2	44.7
HTFETI, averages + moments	$2\cdot2$ subd.	λ_{max}	$2.66\cdot10^{-4}$	$2.64\cdot10^{-4}$	$2.71\cdot10^{-4}$	$2.81\cdot10^{-4}$	$2.80\cdot10^{-4}$	$2.97\cdot10^{-4}$
		λ_{min}^{reg}	$3.29\cdot10^{-6}$	$3.17\cdot10^{-6}$	$3.28\cdot10^{-6}$	$3.29\cdot10^{-6}$	$3.29\cdot10^{-6}$	$3.30\cdot10^{-6}$
		κ^{reg}	80.8	83.2	82.7	85.2	85.1	90.1
	$4\cdot4$ subd.	λ_{max}	$7.10\cdot10^{-4}$	$7.29\cdot10^{-4}$	$6.98\cdot10^{-4}$	$4.62\cdot10^{-4}$	$4.61\cdot10^{-4}$	$8.20\cdot10^{-4}$
		λ_{min}^{reg}	$3.29\cdot10^{-6}$	$3.18\cdot10^{-6}$	$3.29\cdot10^{-6}$	$3.29\cdot10^{-6}$	$3.29\cdot10^{-6}$	$3.30\cdot10^{-6}$
		κ^{reg}	215.6	229.5	212.4	226.0	235.0	248.8
HTFETI, equality in corners	$2\cdot2$ subd.	λ_{max}	$4.80\cdot10^{-4}$	$4.91\cdot10^{-4}$	$5.00\cdot10^{-4}$	$5.19\cdot10^{-4}$	$5.02\cdot10^{-4}$	$5.24\cdot10^{-4}$
		λ_{min}^{reg}	$3.30\cdot10^{-6}$	$3.18\cdot10^{-6}$	$3.29\cdot10^{-6}$	$3.30\cdot10^{-6}$	$3.30\cdot10^{-6}$	$3.30\cdot10^{-6}$
		κ^{reg}	145.8	154.4	152.0	157.3	152.2	158.9
	$4\cdot4$ subd.	λ_{max}	$1.29\cdot10^{-3}$	$1.31\cdot10^{-3}$	$1.28\cdot10^{-3}$	$1.33\cdot10^{-3}$	$1.35\cdot10^{-3}$	$1.40\cdot10^{-3}$
		λ_{min}^{reg}	$3.29\cdot10^{-6}$	$3.18\cdot10^{-6}$	$3.29\cdot10^{-6}$	$3.29\cdot10^{-6}$	$3.29\cdot10^{-6}$	$3.30\cdot10^{-6}$
		κ^{reg}	390.5	413.1	391.1	404.3	410.4	424.1

Table 7: Conditioning of the system matrix $A = PFP$ for TFETI and $A = \tilde{P}\tilde{F}\tilde{P}$ for HTFETI with both tested methods of aggregation for each interconnection variant, for $H = 1/16, H/h = 8$

Finally, convergence properties are better for TFETI than for HTFETI, and for HTFETI and the corresponding method of aggregation, they are better for the case with clusters composed of a lower number of subdomains $(2 \cdot 2)$ than for the case with $4 \cdot 4$ subdomains. Despite the worsening convergence of HTFETI with a growing number of clusters, and compared to TFETI, the overall time of the solution can actually improve due to a smaller and cheaper coarse problem solution.

Looking at the conditioning of the system matrices $A = PFP$ and $A = \tilde{P}\tilde{F}\tilde{P}$ leads naturally to the same conclusions as above for the convergence properties.

5 Conclusions

This work explored all possible variants of gluing subdomain corners for the nonoverlapping domain decomposition methods TFETI and HTFETI on regular 2D domains. We have presented the number of CG iterations and spectral properties for a 2D linear elasticity benchmark.

Both the best spectral and convergence properties are achieved for variant of corners gluing using orthonormal gluing constraints. On the other hand, gluing using fully redundant set of constraints generally performs the worst. There were obtained slightly worse results in terms of both spectral and convergence properties for other variants of gluing, which, however, were cases where the gluing of corresponding quartets of coincident subdomain corners was realised without redundant constraints, i.e. with 3 constraints equating values of one displacement components of one quartet, compared to 6 in fully redundant case, leading to significantly faster performing of mathematical operations in those cases, especially with rising number of subdomains.

Acknowledgements

The authors acknowledge the financial support of the European Union under the REFRESH - Research Excellence For Region Sustainability and High-tech Industries project number CZ.10.03.01/00/22 003/0000048 via the Operational Programme Just Transition. This work was also supported by the the Czech Science Foundation grant 26-20457S and by the European Union through the Operational Programme Jan Amos Komenský under project INODIN, number CZ.02.01.01/00/23_020/0008487. The work was also supported by the SGS grant of VSB-Technical University of Ostrava – Mathematical modeling and algorithm development for computationally intensive engineering problems XII No. SP2026/050.

References

[1] Ch. Farhat, F.-X. Roux ,"A method of finite element tearing and interconnecting and its parallel solution algorithm", International Journal for Numerical Methods in Engineering, 32, 1205-1227, 1991

[2] Z. Dostál, D. Horák, R.Kučera, ”Total FETI - an easier implementable variant of the FETI method for numerical solution of elliptic PDE”, Communications in Numerical Methods in Engineering, 22, 1155-1162, 2006
[3] P. Hrušková, Z. Dostál, O. Vlach, P. Vodstrčil, ”On multipoint constraints in FETI methods”, Applications of Mathematics, 70, 47-64, 2025
[4] A. Klawonn, O. Rheinbach, ”Highly scalable parallel domain decomposition methods with an application to biomechanics”,ZAMM - Journal of Applied Mathematics and Mechanics, 90, 2010
[5] T. Brzobohatý, M. Jarošová, T. Kozubek, M. Menšík, A. Markopoulos. ”The hybrid total FETI method”, Proceedings of the Third International Conference on Parallel, Distributed, Grid and Cloud Computing for Engineering (PARENG), Pécs, Hungary, (Civil-Comp Press, Edinburgh), 137-148, 2013
[6] A. Markopoulos, L. Říha, T. Brzobohatý, P. Jirůtková, R. Kučera, O. Meca, T. Kozubek, ”Treatment of singular matrices in the Hybrid total FETI method”, Domain Decomposition Methods in Science and Engineering XXIII, Conference proceedings, Jeju Island, Korea (Springer Cham), 237-244, 2017
[7] A. Markopoulos; L. Říha; T. Brzobohatý; O. Meca; R. Kučera; T. Kozubek, ”The HTFETI method variant gluing cluster subdomains by kernel matrices representing the rigid body motions”, Domain Decomposition Methods in Science and Engineering XXIV, Conference proceedings, Svalbard, Norway (Springer Cham), 543–551, 2019